THE RICE INSTITUTE

Torsional Creep of Tin at High Temperatures

by

Walter Allan Zama

A THESIS
SUBMITTED TO THE FACULTY
IN PARTIAL FULFILLMENT OF THE
REQUIREMENTS FOR THE DEGREE OF
MASTER OF SCIENCE

Houston, Texas
May, 1960

ABSTRACT

Steady-state creep data are presented for tin tested in torsion at temperatures from 100°C to 228°C. Results obtained below 210°C verify observations of other investigators. A creep activation energy of 22.5 Kcal/mol in this temperature range is determined. Above 210°C, an abnormal increase in the steady-state creep rate is observed. Results are discussed in terms of Weertman's dislocation climb mechanism.

Tertiary-creep data are presented for three temperatures near the melting point. It is observed that the strain at which tertiary creep begins is independent of stress, though highly temperature dependent. These results are discussed in terms of current tertiary-creep and creep-fracture theories.

CONTENTS

INTRODUCTION

It is generally assumed that most engineering materials, such as steel or aluminum, can withstand a constant stress at room temperature indefinitely, as long as the yield stress is not exceeded. However, recent applications, such as turbine blades and missile nose cones, have demanded the use of these materials at higher and higher temperatures until a phenomenon called creep has become important. Creep may be defined as the time-dependent inelastic strain of a material subjected to a constant stress. If a metal specimen at some temperature T has a stress σ applied to it, the specimen will deform and the strain ε can be plotted as a function of time, t. This plot is called a creep curve, Figure 1.

There are three distinct stages of creep:

(a) Primary or transient creep, which includes any initial strain, is characterized by a decreasing strain rate, $\dot{\varepsilon}$. It usually constitutes only a small fraction of the total creep strain.

(b) The steady-state portion follows transient creep, and is so called because $\dot{\varepsilon}$ is constant during this stage.

(c) Steady-state creep is followed by tertiary creep, where ε accelerates until fracture occurs.

Throughout this discussion, the subscripts P, S, and T will denote the primary, steady-state, and tertiary stages

of creep, respectively.

Primary creep has been discussed extensively in the literature. If one disregards the initial instantaneous strain, the primary creep rate can often be represented accurately by the relation

$$\dot{\varepsilon}_P = A\, t^{-n}, \quad 0 < n \leq 1, \tag{1}$$

where A is a function of stress and temperature. When $n = 1$,

$$\varepsilon_P = \varepsilon_o + A \log t. \tag{2}$$

This is called logarithmic creep and is applicable to rubber, glass, and many metals. At faster creep rates and larger strains, n in Equation (1) takes a value closer to 2/3, giving a transient strain law of the type

$$\varepsilon_P = \beta t^{1/3}. \tag{3}$$

This is "beta-creep" and has been discussed extensively by Andrade[1].

Steady-state creep has been comprehensively reviewed by Dorn[2]. He expressed the steady-state creep rate for metals by the following empirical relations:

$$\dot{\varepsilon}_S = G(\sigma) \exp(-Q/RT) \tag{4}$$

$$G(\sigma) = G' \exp(b\sigma) \quad \text{for high stresses}$$
$$G(\sigma) = G'' \sigma^m \quad \text{for low stresses}$$

where G', G", and b are structure-sensitive constants, Q = activation energy for creep, R = universal gas constant, and T = absolute temperature. The activation energy, Q, has been found to have the same value at high temperatures

as the activation energy of self diffusion for most metals. This indicates a dependence of steady-state creep on the diffusion of vacancies.

A theory by Mott[3] and Weertman[4] explains steady-state creep in terms of a dislocation pile-up mechanism. As a material is stressed, Frank-Read sources in the material are activated, and dislocations move in their slip planes. As the dislocations reach barriers, they pile up, creating high stresses on the leading dislocations and back stresses on the sources. These high stresses cause the leading dislocations to "climb" over the barriers. A steady-state situation is reached in which the number of dislocations climbing just equals the number being produced by the sources. The barriers to dislocation movement are sessile dislocations. Under the influence of temperature and stress, dislocations circumvent these obstacles by climbing into new slip planes. Such climbing requires the production or annihilation of vacancies, so that vacancy diffusion becomes the rate-determining factor. Calculations based on this model predict a creep rate at low stresses of:

$$\dot{\varepsilon}_S = B\,\sigma^m \exp\,(-Q/RT), \quad m \sim 4.6. \qquad (5)$$

This is in agreement with Equation (4) for low stresses. This model will form the basis for discussion in this thesis.

There is a dearth of quantitative data on tertiary creep. This stage of creep is usually thought to be a process leading to fracture. Most studies of it are concerned with the formation and propagation of small cracks in the metal, either due to stress concentration or void formation through condensation of vacancies. Since tertiary creep is primarily a high-temperature phenomenon, most investigations have been limited to temperatures greater than 75% of the absolute melting temperature, and have been restricted to relatively small stresses. At present, none of the theories has successfully explained the tertiary-creep behavior of metals.

The purpose of this investigation was to test the validity of presently accepted creep concepts at temperatures approaching the melting point. At the same time, data on high-temperature tertiary creep were to be collected to offer an insight into its mechanism.

Tin was chosen as the material for this investigation primarily for reasons of experimental convenience. Its low melting temperature and ready availability are particularly desirable features. Furthermore, creep data for tin over wide temperature ranges have been published and permit comparison with experimental results obtained in this investigation.

EQUIPMENT AND PROCEDURE

Specimens were tested in torsion, thereby eliminating variation of cross section during the test. This also simplified the maintenance of a uniform temperature along the length of the specimen. The specimens were heated in a small resistance furnace, Figure 2, which was operated at constant current. The furnace was surrounded by a constant-temperature oil bath to isolate it from external temperature variations. With this equipment it was possible to reduce temperature fluctuations to a maximum of 0.3°C with less than 0.3°C variation along the entire length of the specimen. All temperature measurements were made in the center of the specimen with a calibrated copper-constantan thermocouple in conjunction with a Leeds and Northrup potentiometer.

A constant torque was applied to the specimen through a weight and pulley. The angular deformation, θ, produced by the torque was converted into linear motion by a micrometer screw. The latter moved the core of a differential transformer which, in turn, activated a Sanborn recorder. This instrument recorded the angle of twist, θ, as a function of time, t, with a maximum sensitivity of 0.05 radian at full scale deflection, 50 mm, on the recorder chart. The equipment was calibrated prior to each test.

The specimens were prepared by casting commercial tin in steel molds. They were then machined to the dimensions given in Figure 2. Spectrographic analysis of a number of specimens revealed them to be of 99.30% purity, with the following major impurities: 0.51% Pb, 0.09% Sb, and 0.06% As. The grain size was approximately 50 grains per cm^2 before straining.

In carrying out the experiments the specimens were placed into the furnace and allowed to reach the testing temperature. The load was applied gradually by hand. Test runs lasted anywhere from twenty seconds to one hour. Since the results obtained by this method were expressed in terms of the angle of twist as a function of time at constant torque, it was necessary to convert the data into conventional terms of shear stress and strain. Under the assumption that the deformation was one of pure torsion, an equation was developed (see Appendix) by means of which the shear stress at the surface of the specimen could be calculated. It was found that a constant torque was very nearly equivalent to a constant stress.

RESULTS

In Figure 3, steady-state creep rates at different torques are plotted as a function of the reciprocal temperature. At temperatures below about 210°C, the steady-state creep rates at constant torques followed closely the established relation given in Equation (4). The activation energy for this temperature range was found to have a value of $Q = 22.5 \pm 1.0$ Kcal/mol. This is in good agreement with the findings of several investigators. Frenkel, Sherby, and Dorn[5] found $Q = 21.0 \pm 2.0$ Kcal/mol, while Wiseman, Sherby, and Dorn[6] found $Q = 23.0$ Kcal/mol. Weertman and Breen[7] and Weertman[4], whose observations were made with both polycrystals and single crystals of tin, observed $Q = 22.0$ Kcal/mol. The most recent investigations of the creep of tin have been made by Bonar and Craig[8]. Their results, however, were obtained at low temperatures, where a much lower activation energy is usually observed. At temperatures below 210°C, Q appeared to be independent of stress, degree of strain, and temperature, as is the case with the usual creep behavior of metals[2].

At temperatures above about 210°C the results indicated that the Arrhenius-type equation is no longer applicable. Judging from the high-temperature portions of the curves in Figure (3), the process can no longer be

viewed as one having a single activation energy. The slope of the curves tends toward very high values as the melting point is approached. The only other creep results in the high-temperature region with polycrystalline tin are those by Breen and Weertman[9]. The few data collected by those authors in the range near the melting point are not sufficient to corroborate or contradict the results given in Figure 3.

Creep rates at constant temperatures, as a function of stress, are shown in Figure 4. Data for this diagram were obtained from the curves in Figure 3, since it was difficult to repeat tests for different torques at identical temperatures. By and large, the exponential expression by Dorn,

$$\dot{\varepsilon}_S = A(T)\,\sigma^m,$$

is consistent with the results given in Figure 4. In this equation A(T) is a temperature-dependent constant. The values for the exponent m varied from 3.6 to 4.4. Attempts were made to extend the observations of the stress-creep relationship in a more definite way to temperatures even closer to the melting point. This was not possible because steady-state creep data could be obtained only for very small torques. Higher torques were precluded due to the extremely short duration of the high-temperature runs.

In Figures 5, 6, and 7, actual high-temperature creep curves are shown. They all still exhibit a definite linear portion. Yet, as the temperature rises, this steady-state portion tends to take up an increasingly smaller part of the entire creep curve, while the primary-creep portion virtually disappears. In the immediate vicinity of the melting point (at 228°C, not shown) it became very difficult to distinguish between secondary and tertiary creep. Tertiary-creep data at lower temperatures were sought, but the deformation before reaching tertiary creep became excessive, so that the range of validity of Equation (A1) in the Appendix was exceeded.

A striking observation is that the strain at which tertiary creep starts, θ_T, appears to be independent of torque, although it is highly temperature dependent. A similar observation was made by Feltham[10] with steel wires tested in tension. Andrade[11], who worked with lead, interpreted tertiary creep as a recrystallization phenomenon. He expressed the strain at which recrystallization started during creep by

$$\varepsilon_R = C\,\sigma^{1.6}, \qquad (6)$$

where C was a constant independent of temperature. An attempt was made in this investigation to determine whether recrystallization was actually occuring at the onset of tertiary creep. Several specimens were strained

in creep to a twist angle just below that at which tertiary creep begins, θ_T. They were then carefully cut, polished by hand, and etched. Likewise, several specimens were strained in creep past θ_T, polished, and etched. As shown in Figure 9, distortion, but not a change in grain size, occurred during tertiary creep. From several such examinations it was concluded that the initiation of tertiary creep was independent of recrystallization.

An attempt was also made to observe grain boundary sliding. Several specimens were marked lightly with a razor blade on their surface and then strained in creep by various amounts. Microscopic analysis revealed no gross grain boundary sliding.

DISCUSSION

The steady-state creep data discussed in the results are best explained in terms of Weertman's dislocation-climb model. Results obtained at temperatures below 210°C verify observations of other investigators. The B term in Weertman's Equation (5) is slightly temperature-dependent, so that the data of Figure 3 should actually be replotted to account for this temperature-dependence. According to Weertman's original equation, B is inversely proportional to G^3T, where G is the shear modulus and T is the absolute temperature. Köster[12] has given data for the elastic modulus, E, of tin as a function of temperature. Assuming that E/G is independent of temperature, a correction factor, $(G/G_o)^3\ (T/T_o)$, may be obtained from these data. G_o is just a convenient reference value of the shear modulus at T_o = 373°K. This correction factor was multiplied by the creep rates given in Figure 3, and the results were plotted in Figure 10. The only significant change in the data was a lowering in the activation energy from 22.5 Kcal/mol to 21.2 Kcal/mol.

Steady-state creep rates obtained at temperatures above 210°C exhibit a departure from ordinary creep behavior. The unusual increase in the creep rate near the melting point may suggest a breakdown of the barriers holding the dislocation pile-ups. Stroh[13] proposes that

sessile dislocations might break down under the combined effects of high temperature and stress. Should this occur to a portion of the barriers, the effective length of piled-up groups of dislocations would increase. According to Weertman's formulation, the creep rate should be proportional to the square of this length, so that the breakdown of sessile dislocations would enhance the creep rate. Due to the uncertainty of this hypothesis, a quantitative analysis is not justified.

In Weertman's analysis, the vacancy diffusion coefficient is a rate-determining factor. An unusual increase in this coefficient near the melting point could account for the high-temperature data of Figure 3. Such an increase is unlikely, however, as indicated by the work of Eckert and Drickamer[14]. They studied the self-diffusion rate of indium near the melting point, and observed an increase only within 1°C of the melting temperature.

The possibility that impurity atoms might be clustering at grain boundaries so as to cause there a lowering of the melting temperature was considered. Weinberg and Teghtsoonian[15] showed, however, that 0.4% Pb impurity in tin lowers the grain-boundary melting temperature only about 1°C. This work, plus the absence of any observable grain-boundary slip on the surface of the specimens used in this investigation, make such a possibility unlikely.

Many investigators have observed that tertiary creep is accompanied by the presence of small micro-cracks along grain boundaries normal to the tensile stress direction. This has led to the proposal of many models of tertiary creep based on crack formation and crack propagation. Buffington and Cohen[16] contend that a high stress concentration is necessary for void formation. Such stress concentrations may be found at grain boundaries. Kochendörfer[17] has provided a mechanism for the formation of cracks based on dislocations alone. In his theory, dislocations are forced together during the loading of the specimens, opening cracks during the beginning of creep. On the other hand, Crussard and Friedel[18] have chosen to explain the mechanism in terms of vacancies alone. Small cracks, initiated during primary creep, grow by the addition of vacancies, which diffuse to the cracks. When a critical size is reached, the crack propagates through the material. More recently, Hull and Rimmer[19] have developed a theory of crack failure based on vacancy diffusion along grain boundaries. They adopt a Griffith-crack[20] criterion which leads to the following expression for the time to rupture as a function of stress:

$$t_r \sim F(T)/\sigma - P, \qquad (7)$$

where F(T) is a function of temperature, σ = externally applied stress, and P = hydrostatic pressure. These

authors present data for copper that corroborate their theory over a limited stress and temperature range.

In this investigation, small cracks were observed along grain boundaries after tertiary creep. In order to determine whether the Hull-Rimmer mechanism of vacancy diffusion was the prevailing one, a curve of log t_T vs. log σ was plotted from the data of Figure 5. The slope was found to be constant and equal to -4.7. Comparison with Equation (7) shows that t_T is much more stress-dependent than it would be for a vacancy mechanism.

The data of Figures 5-7 suggest that strain is an important parameter. An attempt to explain these data in terms of a pile-up mechanism follows: The specimen is stressed and begins to creep. The rate-determining factor is dislocation climb. Each element of creep strain is due to one dislocation's climbing over one barrier. At low stresses, however, grain boundaries offer an insurmountable barrier to climb[13,21]. Hence, dislocations start piling up on slip planes at grain boundaries, causing a high stress concentration there. This stress may become large enough to propagate existing microcracks. When this happens, the material able to withstand the applied load is reduced, so that the effective applied stress is increased. Eventually this leads to catastrophic creep and failure.

A check on the validity of this proposed mechanism was made by creeping specimens to a strain just below θ_T,

reversing the torque, and observing the strain at which tertiary creep was initiated, Figure 8. When the torque was reversed, a high initial creep rate was observed. This could be due to the unpiling of the dislocations. As the strain crossed the zero point, all trace of the previous creep had disappeared, and the specimen went on into tertiary creep at the same θ_T as in an ordinary test.

An analysis by Stroh[22] lends itself well to this formulation. Stroh considers the stress produced by a pile-up of n dislocations at an obstacle. This pile-up causes a stress concentration large enough to propagate a crack whenever $n \geq n^*$, n^* being given by

$$n^* = 12s/b\sigma. \tag{8}$$

In this equation, s = surface tension = 685 dynes/cm for tin at 215°C[23], σ = applied shear stress, in dynes/cm^2, and b = Burgers vector = 3×10^{-8} cm. Stroh's analysis was chosen since the cracks observed in this investigation were parallel to the grain boundaries. A similar analysis was made by Gilman[25] for cracks parallel to the slip plane. If it is assumed that the number of dislocations piling up at a grain boundary is proportional to the strain, and if the steady-state strain rate is taken proportional to σ^4, an equation may be found giving the time at which rupture occurs to be inversely proportional to σ^5. This is in good agreement with the data of Figure 5.

The major objection to this theory is that an absurdly large pile-up would be necessary to cause fracture. For a typical applied stress, 250 psi, Equation (8) gives $n^* =$ 16,000 dislocations. The length of such a pile-up, calculated from Stroh's analysis, would be about 0.5 cm! If the surface energy, s, is taken as the grain boundary surface energy, rather than the bulk surface energy, a slightly reduced value for n^* would undoubtedly be obtained. The pile-up, however, would still be exceedingly large.

Theoretical interpretations of tertiary creep proposed by various authors have fallen into two catagories. The first, based on void formation by vacancy migration, leads to an incorrect stress dependence. The second, which takes stress concentrations due to dislocation pile-ups into account, at least in the case of tin, leads to unreasonably large pile-ups. Further theoretical work, possibly based on a completely different approach, will be necessary to explain the experimental observations of this investigation.

CONCLUSIONS

1. Commercial tin has a steady-state creep activation energy of 22.5 Kcal/mol at temperatures from 100°C to 210°C.
2. At temperatures approaching the melting point, the simple Arrhenius-type equation is no longer applicable.
3. The strain at which tertiary creep starts is independent of stress, though it is highly temperature dependent.
4. None of the current theories adequately describe the tertiary creep mechanism.

APPENDIX

The following derivation is credited to Mr. J. R. Baker, formerly a graduate student of The Rice Institute. The results are similar to those obtained by Ludwik[24] from the theory of plasticity.

Consider a section of the cylindrical portion of the specimen. At a given temperature, the shear stress at a distance r from the axis, and due to a torque τ, is σ_r. During steady-state creep at a constant temperature it is assumed that σ_r is a function only of r and the creep rate $\dot{\theta}$. It is further assumed that planes perpendicular to the specimen axis remain plane during deformation. Therefore, since the ends of the specimen are rigidly constrained and rotated, there must be at least one cross section of the specimen where the strain is given by $\varepsilon = r\theta/L$, L being the specimen length. Therefore, the following formula can be used to compute the strain rate.

$$\dot{\varepsilon} = r\dot{\theta}/L \tag{A1}$$

The total torque on the specimen is given by

$$\tau = 2\pi \int_a^b \sigma_r \, r^2 \, dr, \tag{A2}$$

where a and b are the inner and outer radii of the cylinder. Since $\sigma_r = \sigma_r(r, \dot{\theta})$, the following partial derivatives may be formed:

$$\left(\frac{\partial \sigma_r}{\partial \dot{\theta}}\right)_r = \left(\frac{\partial \sigma_r}{\partial \dot{\varepsilon}}\right)\left(\frac{\partial \dot{\varepsilon}}{\partial \dot{\theta}}\right)_r = \frac{r}{L}\,\frac{\partial \sigma_r}{\partial \dot{\varepsilon}} \tag{A3}$$

$$\left(\frac{\partial \sigma_r}{\partial r}\right)_{\dot\theta} = \left(\frac{\partial \sigma_r}{\partial \dot\varepsilon}\right)\left(\frac{\partial \dot\varepsilon}{\partial r}\right)_{\dot\theta} = \frac{\dot\theta}{L}\ \frac{\partial \sigma_r}{\partial \dot\varepsilon} \tag{A4}$$

Combining (A3) and (A4), one obtains

$$\left(\frac{\partial \sigma_r}{\partial \dot\theta}\right)_r = \frac{r}{\dot\theta}\left(\frac{\partial \sigma_r}{\partial r}\right)_{\dot\theta} \tag{A5}$$

Hence from (A2),

$$\dot\theta\left(\frac{\partial \tau}{\partial \dot\theta}\right)_r = 2\pi\int_a^b \left(\frac{\partial \sigma_r}{\partial r}\right)_{\dot\theta} r^3\, dr \tag{A6}$$

Adding 3τ to both sides of (A6) gives

$$\begin{aligned}\dot\theta\frac{\partial \tau}{\partial \dot\theta} + 3\tau &= 2\pi\int_a^b \left(\frac{\partial \sigma_r}{\partial r}\right)_{\dot\theta} r^3 dr + 6\pi\int_a^b \sigma_r\, r^2 dr \\ &= 2\pi\int_a^b \frac{\partial(\sigma_r r^3)}{\partial r}\, dr \\ &= 2\pi\left[\sigma_b b^3 - \sigma_a a^3\right],\end{aligned} \tag{A7}$$

where σ_b and σ_a are the stresses evaluated at the outer and inner surfaces of the specimen. Equation (A7) may be put into the following form:

$$\sigma_b - \sigma_a (a/b)^3 = \frac{\dot\theta\frac{\partial \tau}{\partial \dot\theta} + 3\tau}{2\pi b^3} \tag{A8}$$

Since the stress σ_a near the axis of the specimen cannot exceed the stress σ_b on an outer fiber, and since $(a/b)^3 \ll 1$, $\sigma_a(a/b)^3$ may be neglected compared to σ_b. This gives the formula used to compute the stresses shown in Figure 3:

$$\sigma = \sigma_b = \frac{\dot{\theta}\frac{\partial \tau}{\partial \dot{\theta}} + 3\tau}{2\pi b^3} \tag{A9}$$

Tests were run at different values of τ and T so that a curve of τ vs. ln $\dot{\theta}$ could be plotted. The slope gives the first term in the numerator of Equation (A9). At a given torque, it was observed that $\dot{\theta}\frac{\partial \tau}{\partial \dot{\theta}}$ was essentially constant and had a value close to 1.0 lb-in. Any variation in the stress computed for a given torque in this manner was negligible so it was concluded that a constant torque gave a constant stress at all temperatures tested.

SYMBOLS

Symbol	Description	Units
σ	stress	psi
ε	strain	-
$\dot{\varepsilon}$	strain rate	1/sec
τ	torque	lb-in
θ	angle of twist	radian
$\dot{\theta}$	torsional creep rate	rad/sec
Q	activation energy	cal/mol
R	universal gas constant	1.986 cal/mol-^{o}K
T	absolute temperature	^{o}K
r	radius (variable)	inch
a	specimen inner radius	0.0703 inch
b	specimen outer radius	0.2250 inch
L	specimen length	0.8750 inch
θ_T	strain at which tertiary creep starts	radian

REFERENCES

1. E. N. da C. Andrade, "The Concept of Creep," Creep and Recovery, 1957.

2. J. E. Dorn, "Some Fundamental Experiments on High Temperature Creep," Jour. Mech. Phys. Solids, 3 (1954), 85-116.

3. N. F. Mott, "The Mechanical Properties of Metals," Proc. Phys. Soc. London, B-64 (1951), 729-741.

4. J. Weertman, "Theory of Steady-State Creep Based on Dislocation Climb," Jour. Appl. Phys., 26 (1955), 1213-1217.

5. R. E. Frenkel, O. D. Sherby, J. E. Dorn, "Activation Energies for Creep of Cadmium, Indium, and Tin," Acta Met., 3 (1955), 470-472.

6. C. D. Wiseman, O. D. Sherby, J. E. Dorn, "Creep of Single Crystals of Aluminum, Lead, and Tin," Jour. Metals, 9 (1957), 57-59.

7. J. Weertman, J. E. Breen, "Creep of Tin Single Crystals," Jour. Appl. Phys., 27 (1956), 1189-1193.

8. L. G. Bonar, G. B. Craig, "Activation Energy for Creep of Tin," Canadian Jour. Phys., 36 (1958), 1445-1449.

9. J. E. Breen, J. Weertman, "Creep of Polycrystalline Tin," Jour. Metals, 7 (1955), 1230-1234.

10. P. Feltham, "The Plastic Flow of Iron and Plain Carbon Steels above the A_3-Point," Proc. Phys. Soc. London, B-66 (1953), 865-883.

11. E. N. da C. Andrade, "The Flow of Metals," Jour. Iron Steel Inst., 171 (1952), 217-228.

12. W. Köster, "Die Temperaturabhängigkeit des Elastizitätsmoduls reiner Metalle," Zeit. für Metallkunde, 39 (1948), 1-9.

13. A. N. Stroh, "The Strength of Lomer-Cottrell Sessile Dislocations," Phil. Mag., Ser. 8, 1 (1956), 489-502.

14. R. E. Eckert, H. G. Drickamer, "Diffusion in Indium Near the Melting Point," Jour. Chem. Phys., 20 (1952), 13-17.

15. F. Weinberg, E. Teghtsoonian, "Grain-Boundary Melting," Acta Met., 5 (1957), 455-464.

16. F. S. Buffington, M. Cohen, "Self-Diffusion in Alpha Iron under Uniaxial Compressive Stress," Trans. Amer. Inst. Min. Met. Engr., 194 (1952), 859.

17. A. Kochendörfer, "A Theory of Brittle and Ductile Fracture with Application to Creep Fracture, Based on the Dynamic Behavior of Dislocations and Condensation of Vacancies," Creep and Fracture of Metals at High Temperatures, 1956, London.

18. C. Crussard, J. Friedel, "Theory of Accelerated Creep and Rupture," Creep and Fracture of Metals at High Temperatures, 1956, London.

19. D. Hull, D. E. Rimmer, "The Growth of Grain Boundary Voids under Stress," Phil. Mag., Ser. 8, 4 (1959), 673-687.

20. A. A. Griffith, "The Phenomena of Rupture and Flow in Solids," Phil. Trans. Roy. Soc., A-221 (1921), 163-198.

21. E. Orowan, "Crack Length Interpreted with the Aid of Plastic Glide," International Conference on Physics, London, 1934.

22. A. N. Stroh, "The Formation of Cracks as a Result of Plastic Flow," Proc. Roy. Soc. London, A-223 (1954), 404-414.

23. The Properties of Tin, Tin Research Institute, March, 1954, England.

24. O. Hoffman, G. Sachs, Introduction to the Theory of Plasticity for Engineers, McGraw Hill, 137-139.

25. J. J. Gilman, "Fracture of Zinc-Monocrystals and Bicrystals," Trans., Met. Soc. AIME, 212 (1958), 783-791.

ACKNOWLEDGEMENTS

I would like to acknowledge gratefully the help and suggestions of Dr. F. R. Brotzen, without whom this thesis would not have been possible. Acknowledgement is also made to the Army Ballistic Missile Agency, Huntsville, Alabama, for its sponsorship of the project under contract number DA-23-072-ORD-1167, and to the National Aeronautic and Space Administration for financial support in the later stages of the project.

FIGURES

FIGURE 1: A TYPICAL CREEP CURVE

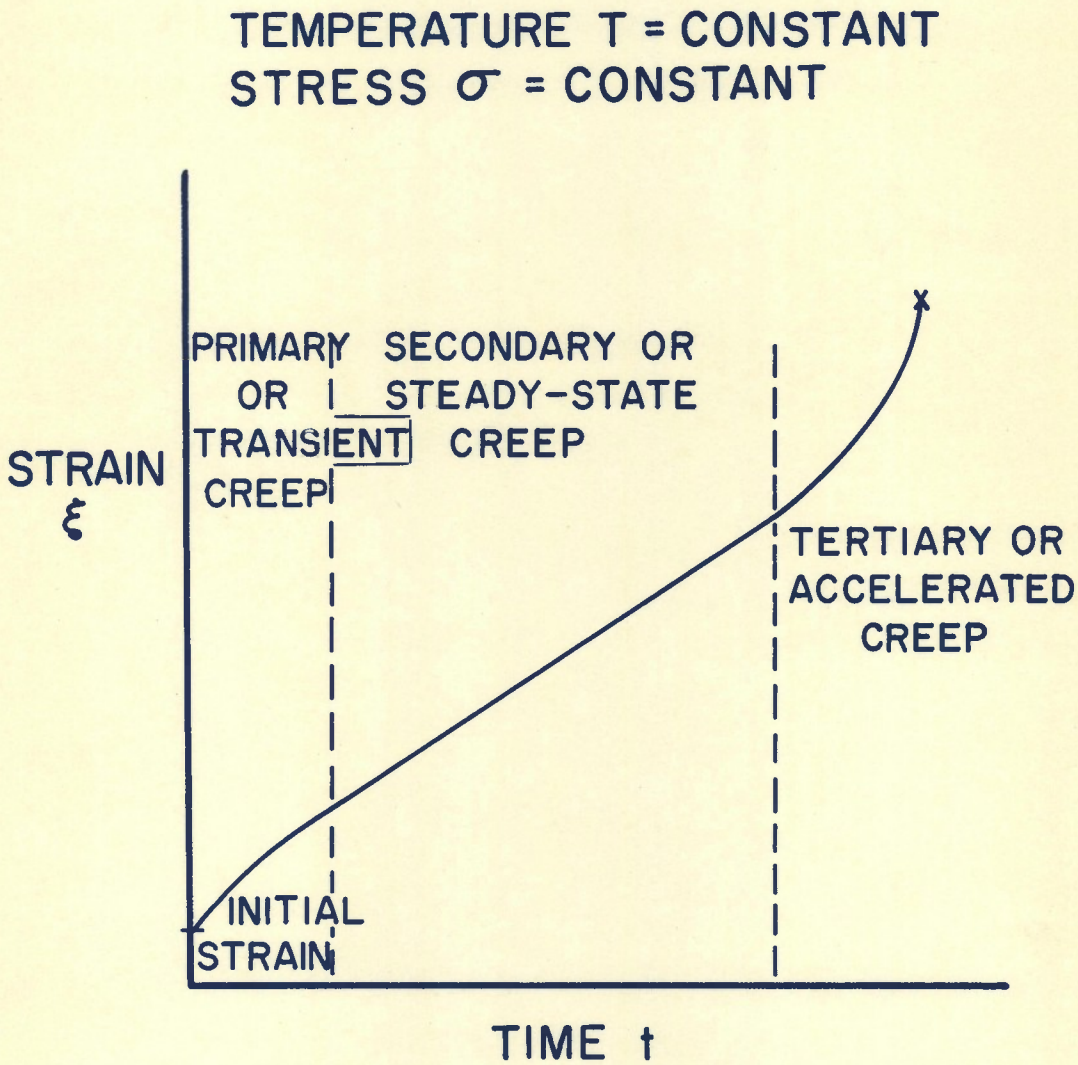

FIGURE 2: TORSIONAL CREEP TESTING MACHINE AND SPECIMEN

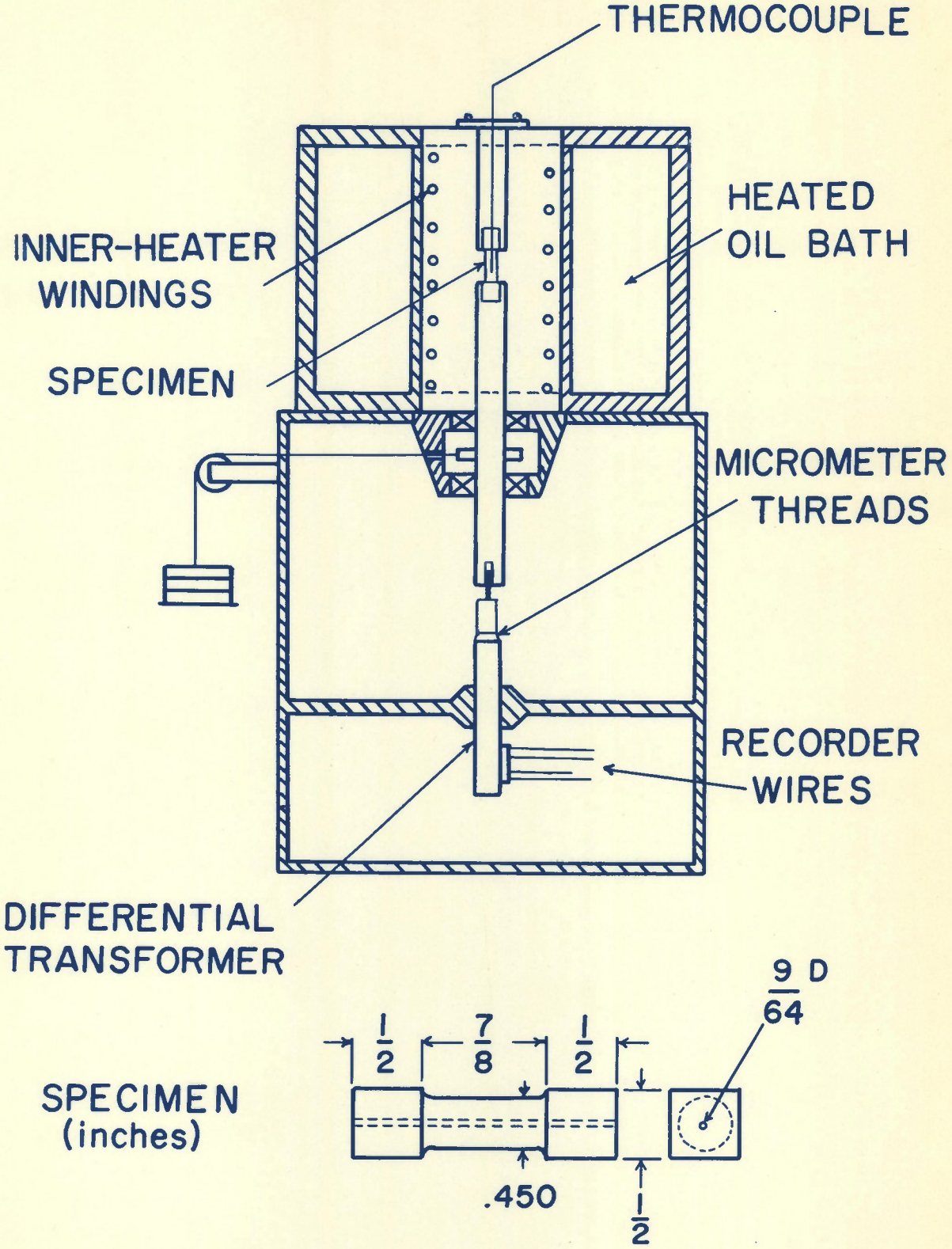

FIGURE 3: STEADY-STATE CREEP RATES AT DIFFERENT TORQUES AS A FUNCTION OF TEMPERATURE

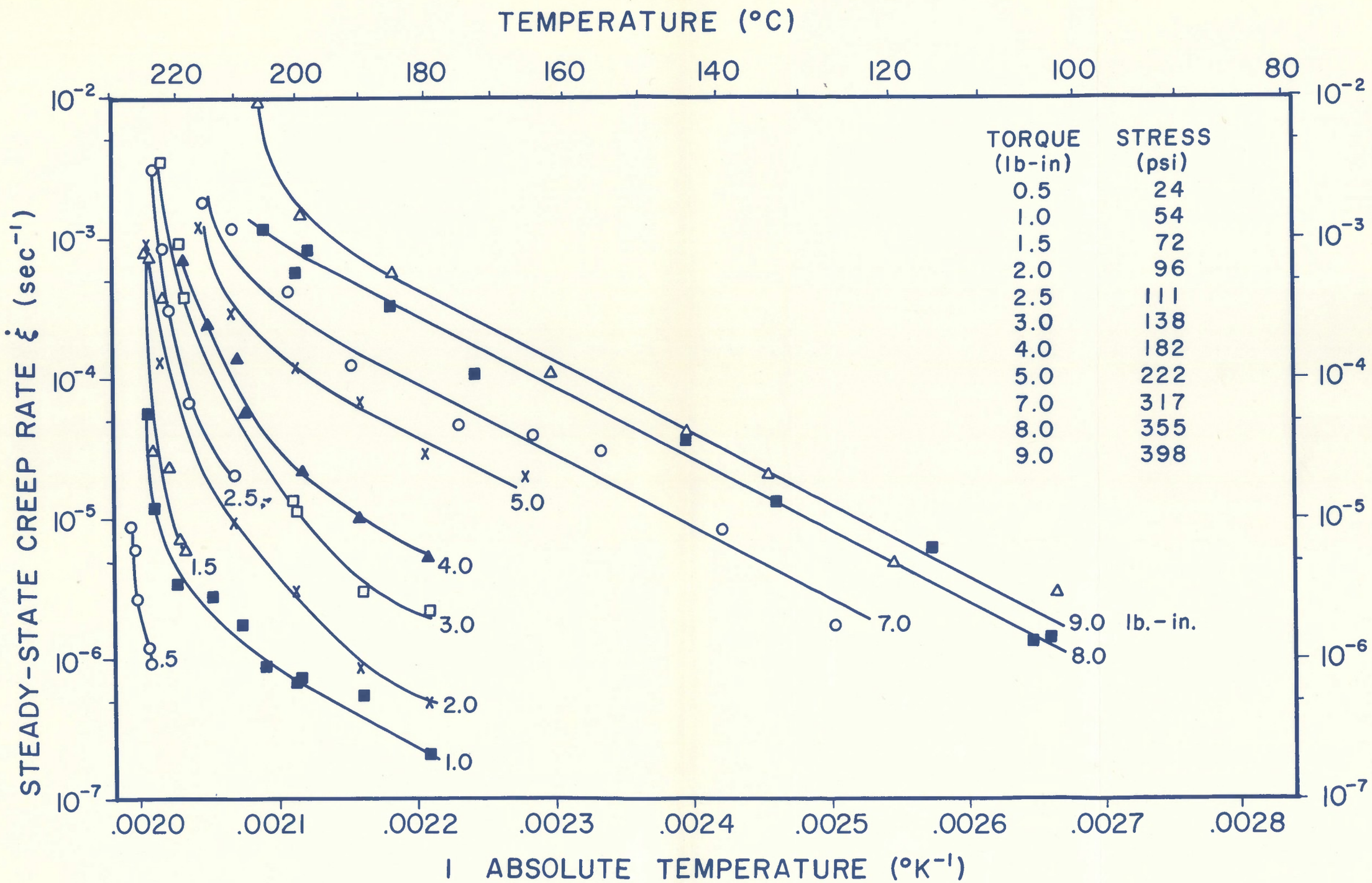

FIGURE 4: LOGARITHMIC PLOT OF STEADY-STATE CREEP RATE VS. STRESS

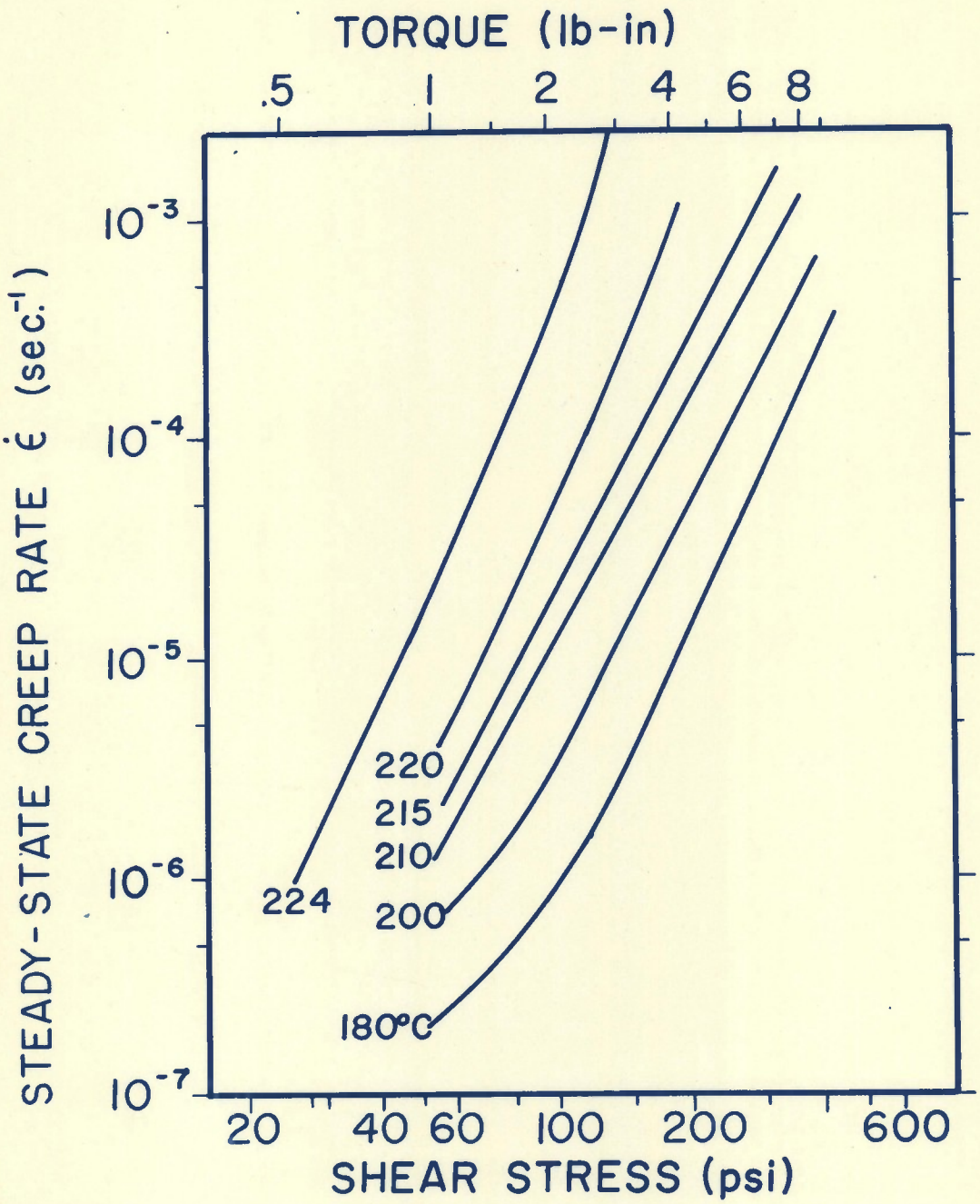

FIGURE 5: DATA AT 215° C

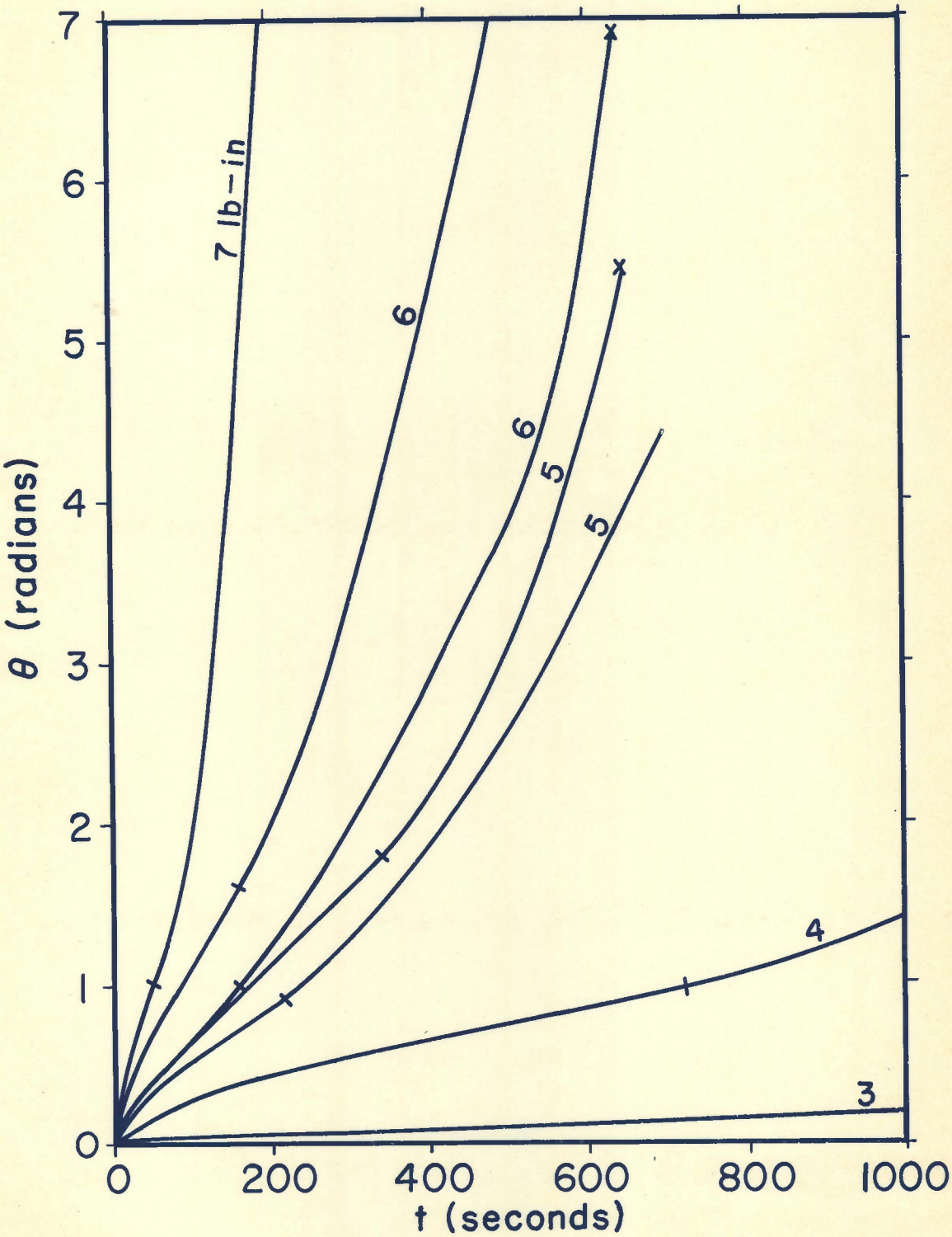

FIGURE 6: DATA AT 220° C

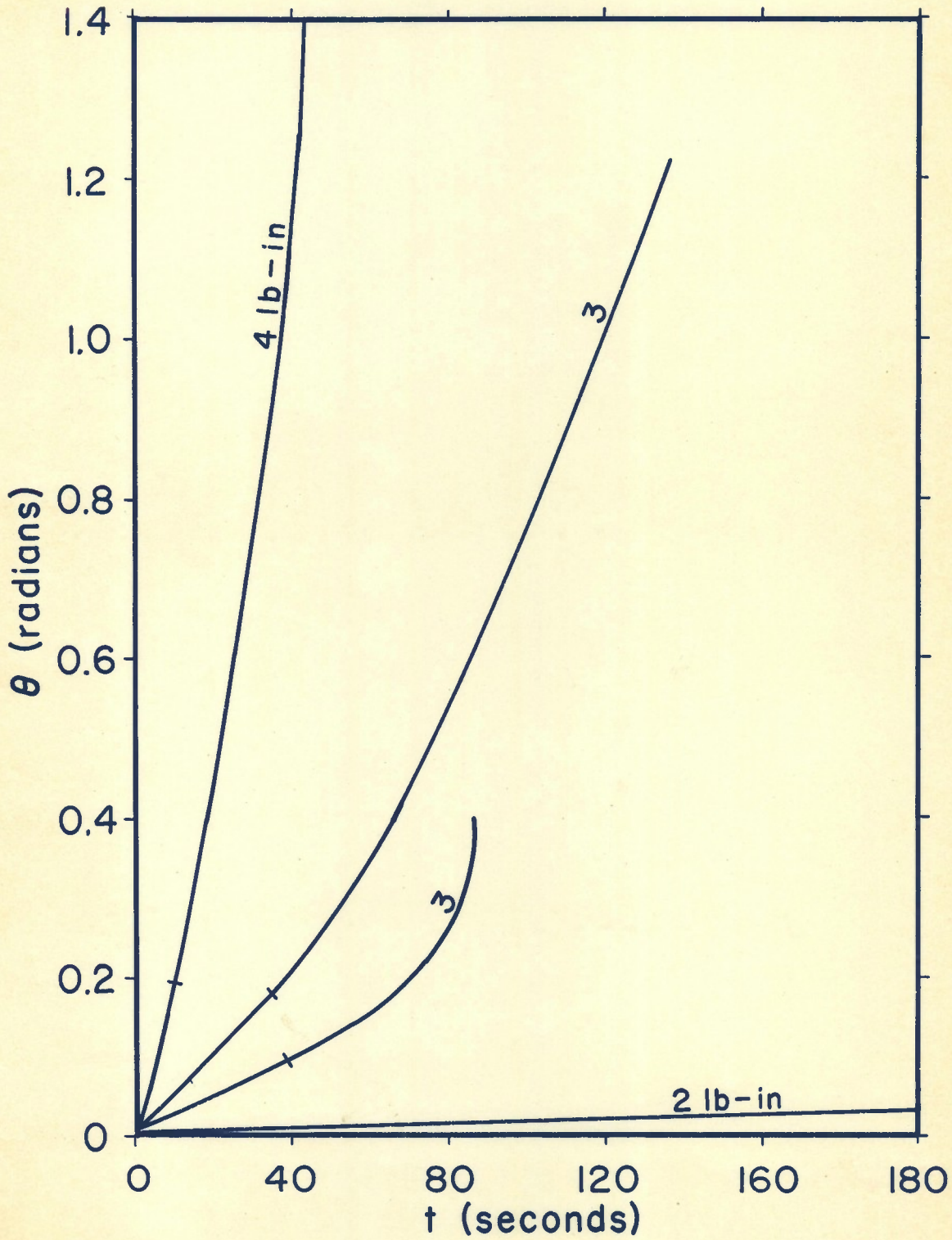

FIGURE 7: DATA AT 224° C

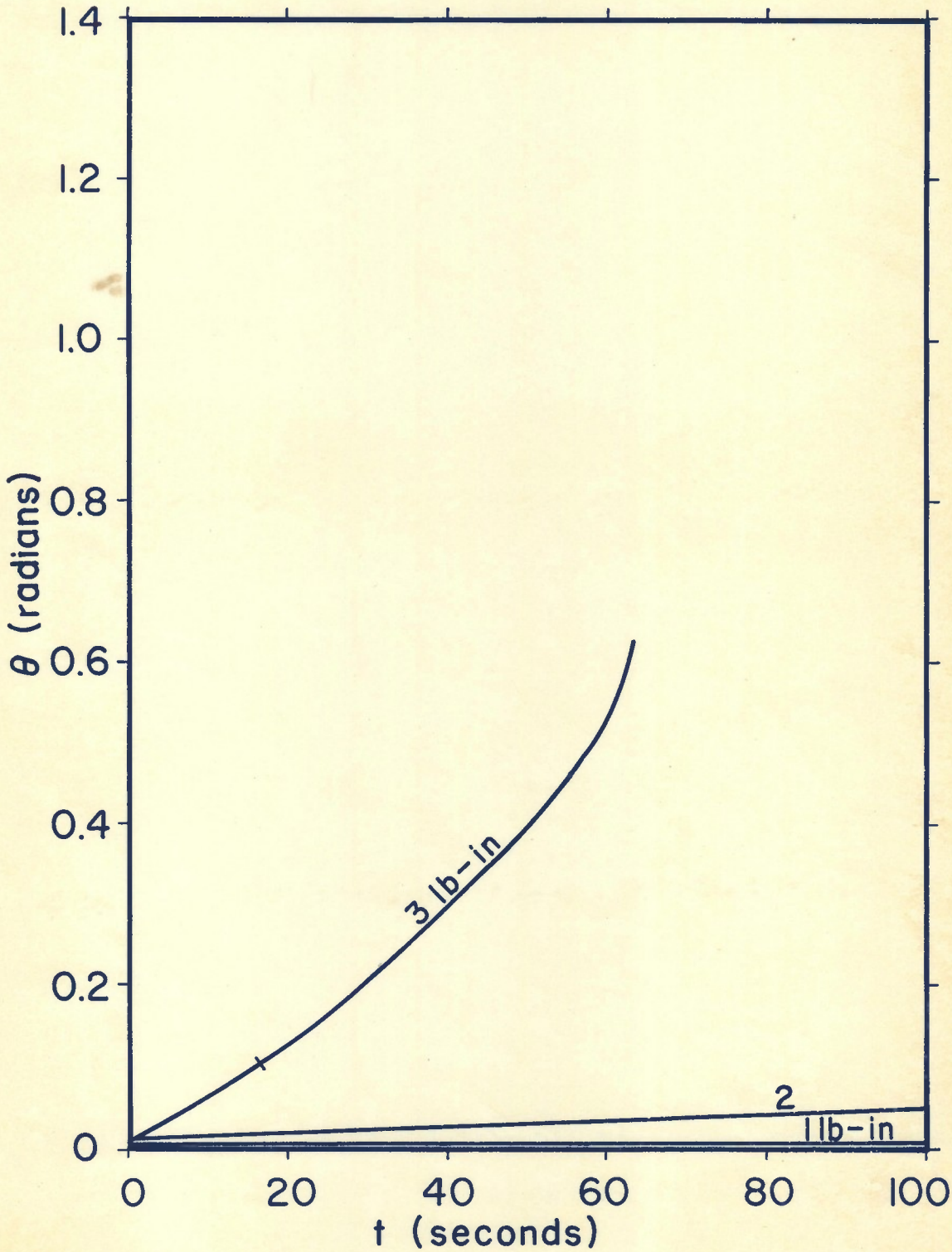

FIGURE 8: REVERSED TORQUE DATA

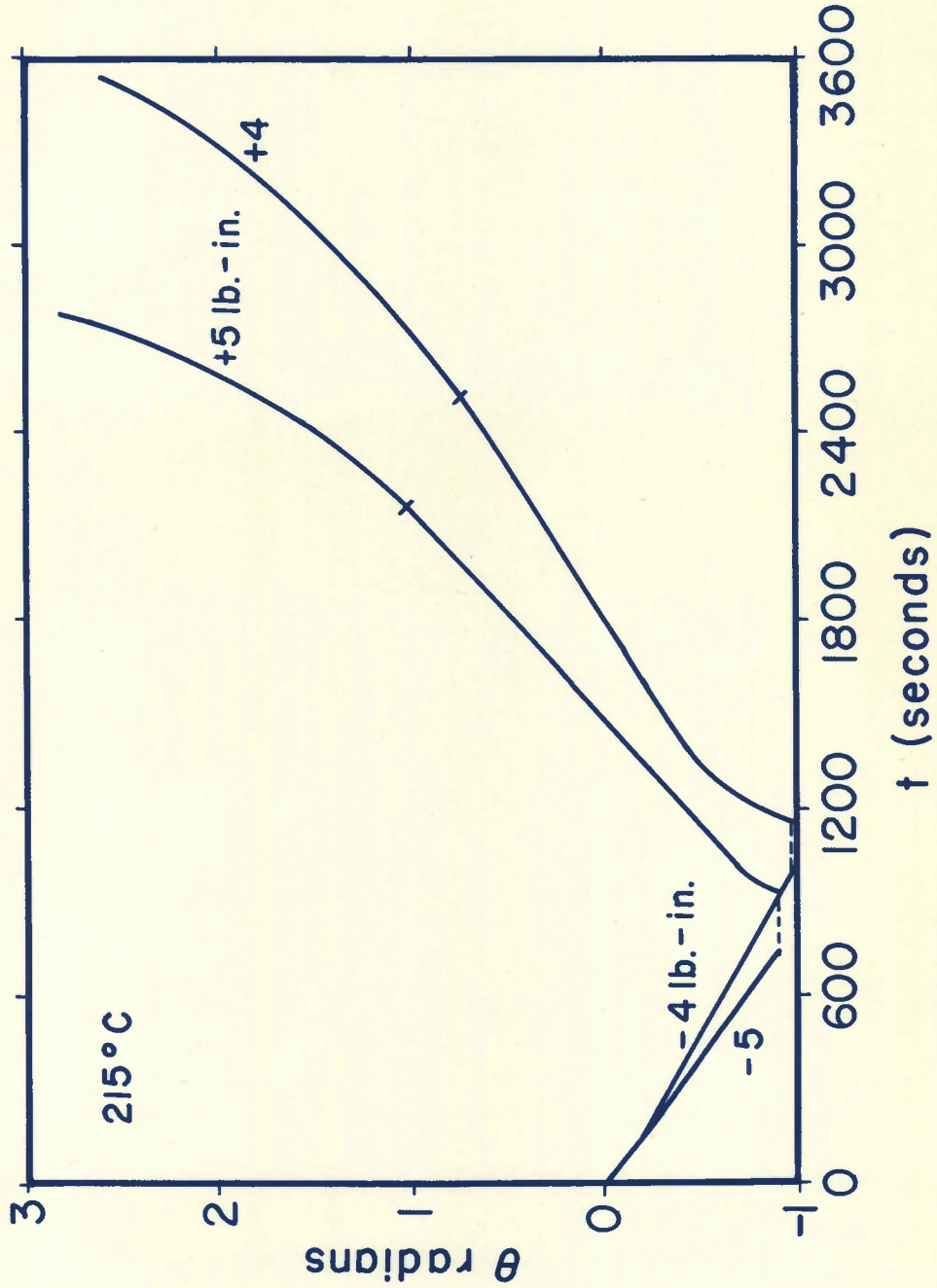

FIGURE 9: GRAIN STRUCTURE AFTER CREEP

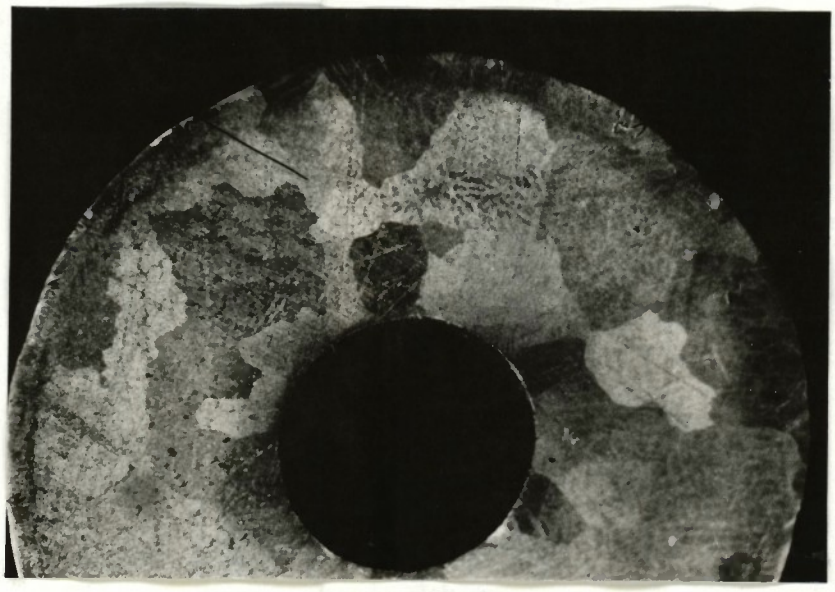

STEADY-STATE CREEP 215°C

TERTIARY CREEP 215°C

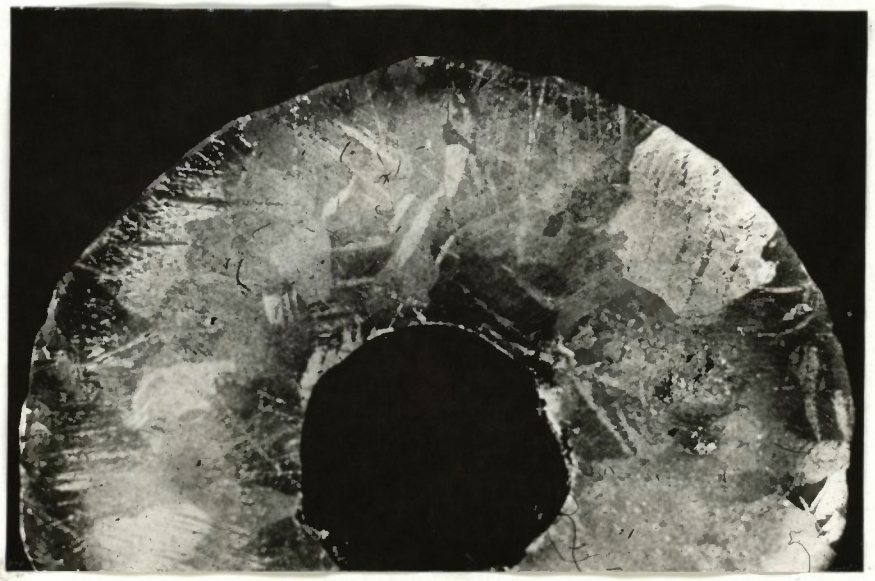

FIGURE 10: LOG ($TG^3\dot{\xi}$) VS. 1/T FOR DIFFERENT TORQUES